Transport properties of electron-doped $La_{2-x}Ce_xCuO_4$ cuprate thin films

H. Wu,[1] L. Zhao,[1] J. Yuan,[1] L. X. Cao,[1] J. P. Zhong,[1] L. J. Gao,[1] B. Xu,[1] P. C. Dai,[2] B. Y. Zhu,[1] X. G. Qiu,[1] and B. R. Zhao[1,*]

[1]*National Laboratory for Superconductivity, Institute of Physics and Beijing National Laboratory for Condensed Matter Physics, Chinese Academy of Sciences, Beijing 100080, People's Republic of China*

[2]*Department of Physics and Astronomy, The University of Tennessee, Knoxville, Tennessee 37996–1200, USA*

(Received 21 April 2005; revised manuscript received 22 November 2005; published 24 March 2006)

Electron-doped $La_{2-x}Ce_xCuO_4$ ($x=0.06-0.20$) thin films with two orientations (100) and (103) were successfully grown and their transport properties were investigated. It is found that the temperature dependence of the in-plane resistivity ρ_{ab} evolves from semiconducting behavior for underdoped films to two-dimensional Fermi liquid behavior for optimally and overdoped ones, while the *c*-axis resistivity ρ_c shows nonmetallic behavior except for heavily overdoped films. The doping-dependent anisotropy factor ρ_c/ρ_{ab} is found to vary from 60 to 1500 at 50 K, and the largest anisotropy value related to the highest T_C is obtained at the optimal doping ($x=0.10$).

DOI: 10.1103/PhysRevB.73.104512 PACS number(s): 74.25.Fy, 72.15.Eb, 74.78.Bz, 74.72.Dn

I. INTRODUCTION

The anisotropy of the transport properties, ρ_c/ρ_{ab}, in high-T_C superconductors (HTSCs) remains to be understood theoretically and experimentally.[1–13] The reason is the complication of the transport properties mainly in the *c*-axis direction, which are very different from the acknowledged behavior of ρ_{ab}. Therefore, to promote the study of this topic, a systematic study of ρ_{ab} and ρ_c on HTSC samples with various doping levels is very necessary.

Due to the relatively low T_C and the high quality electron-doped HTSCs are more difficult to synthesize, most experimental studies on the transport properties have been carried out in the hole-doped (*p*-type) HTSCs,[5–9] and only a few works address the electron-doped (*n*-type) ones. Structurally, the typical electron-doped cuprates are T' phase, and the apical oxygen which characterizes the hole-doped HTSCs is absent. This leads to some essential difference between these two kinds of superconductors. Until now, most experimental studies on the electron-doped cuprates have been performed in the $L_{2-x}Ce_xCuO_4$ (L=Pr,Nd, etc.) system, especially $Nd_{2-x}Ce_xCuO_4$ (NCCO),[10–13] because it is relatively easy to fabricate a high-quality single crystal of NCCO at present. Another electron-doped compound in this T'-phase system, $La_{2-x}Ce_xCuO_4$ (LCCO),[14–16] is somewhat special, since La^{3+} is the only cation that is larger than Ce^{4+} in this kind of compound, and LCCO has the highest transition temperature in all known T'-phase HTSCs, in which some other new features can be expected.[15] However, the T' phase in LCCO is a metastable phase and it can only be synthesized at relative lower temperature comparing to the other T'-phase $Ln_{2-x}Ce_xCuO_4$ materials. Therefore, it is very difficult to fabricate single-phase bulk T'-phase LCCO,[14] and the growth of single-crystal T'-phase LCCO is almost impossible at present.[17] Fortunately, LCCO in the T' phase with expected orientations can be prepared in epitaxial thin films, which is the only way to investigate the anisotropic features of LCCO.

In the present work, $La_{2-x}Ce_xCuO_4$ ($0.06 \leqslant x \leqslant 0.20$) thin films were prepared by dc magnetron sputtering. The (001) LCCO films used to study the *ab*-plane transport properties were grown on (100) $SrTiO_3$ (STO) substrates, while (103) LCCO films used to examine out-of-plane transport properties were grown on miscut (110) STO substrates. The results show that both ρ_{ab} and ρ_c change from nonmetallic to metallic behavior with the increase of Ce concentration from the underdoped to the overdoped (heavily overdoped for ρ_c) regions, though their temperature dependence behaviors are different. The large anisotropy obviously correlates with the two-dimensional (2D) nature in LCCO.

II. SAMPLE PREPARATION

Stoichiometric targets of LCCO were synthesized by a conventional solid state reaction, and the details of the preparation of the thin films can be found in Ref. 18. The pure T' phase with perfect crystallization can be obtained only under the optimal deposition conditions and with the proper concentration of Ce and Cu. Since the substitution of Ce^{4+} for La^{3+} can reduce the perovskite crystallographic Goldschmidt tolerance factor *t* and increase the stabilization temperature of the T' phase, the larger Ce concentration in LCCO will lead to higher optimal deposition temperature.[19,20] In fact, we have found that the optimal deposition temperature increases from 625 °C for the underdoped films to 710 °C for the overdoped films, and the deposition temperature for the optimally doped samples, $x=0.10$, is about 700 °C. The base pressure of the vacuum chamber prior to deposition was below 3×10^{-4} Pa. The deposition gas is a mixture of high-purity argon and oxygen with a ratio of O_2 to Ar 1:4, and the total pressure is 40 Pa. The thicknesses of all samples are restricted in the range of 150–200 nm. After deposition, the samples were cooled down and annealed at about 600 °C in vacuum for about 30 min to remove the excess apical oxygen.

To systematically investigate the in-plane and out-of-plane resistivity ρ_{ab} and ρ_c, (001)-oriented samples grown on (100) STO substrates and (103)-oriented samples grown on (110) STO substrates were prepared, respectively. In order to

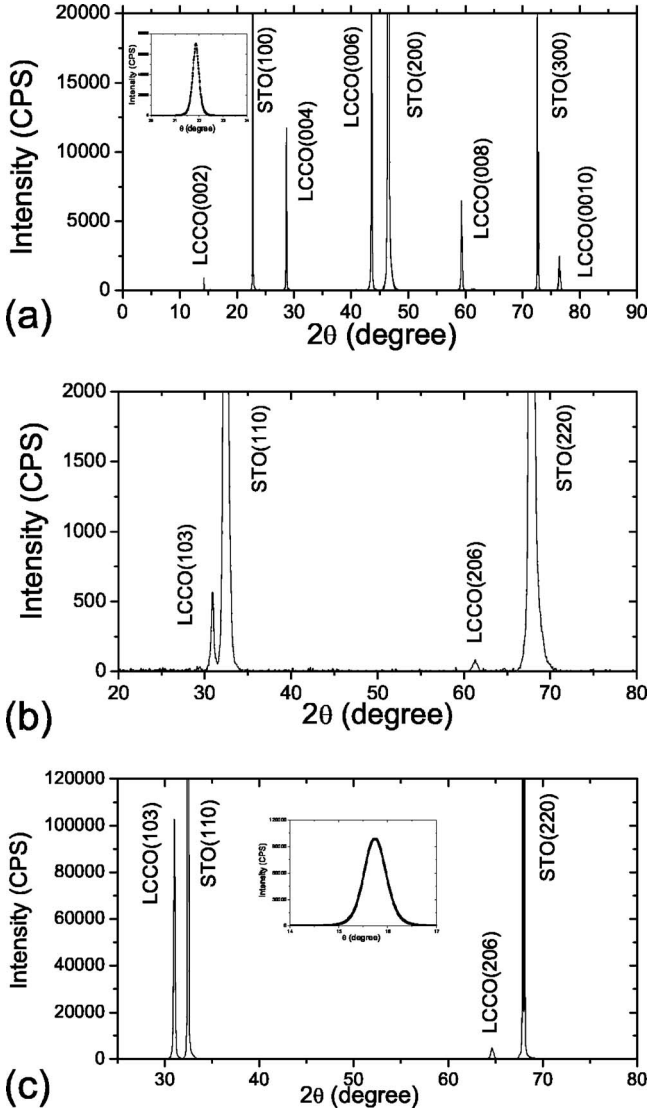

FIG. 1. XRD spectra of the optimally doped samples. (a) (001) LCCO; the inset shows the rocking curve of the (006) peaks. (b) (103) LCCO grown on (110) STO substrate. (c) (103) LCCO grown on miscut (110) STO substrate, where the intensity is orders of magnitude larger than the case of (103) LCCO grown on (110) STO substrate. The inset shows the rocking curve of the (103) peaks.

make more reasonable comparison of ρ_{ab} and ρ_c, each pair of (001)- and (103)-oriented LCCO thin films was prepared in the same batch to acquire the same Ce concentrations.

X-ray diffraction (XRD) analysis was performed for the samples. Figure 1(a) presents the XRD θ-2θ pattern of the (001)-oriented LCCO films at the optimal Ce concentration $x=0.10$, and the inset shows the rocking curve of the (006) peaks. The full width at half maximum (FWHM) is $\sim 0.27°$. This indicates that the films of the *c*-axis-oriented phases are of high quality.

Similar to the $La_{2-x}Sr_xCuO_4$ (LSCO) thin films grown on the (110) STO substrate,[23] there are two kinds of domains, (103) and (103)′ in LCCO films,[24] and the (103)′ domain is the mirror image of the (103) domain. These two degenerate inherent domains have opposite normal directions of their CuO_2 planes. Hence there will be lots of domain boundaries

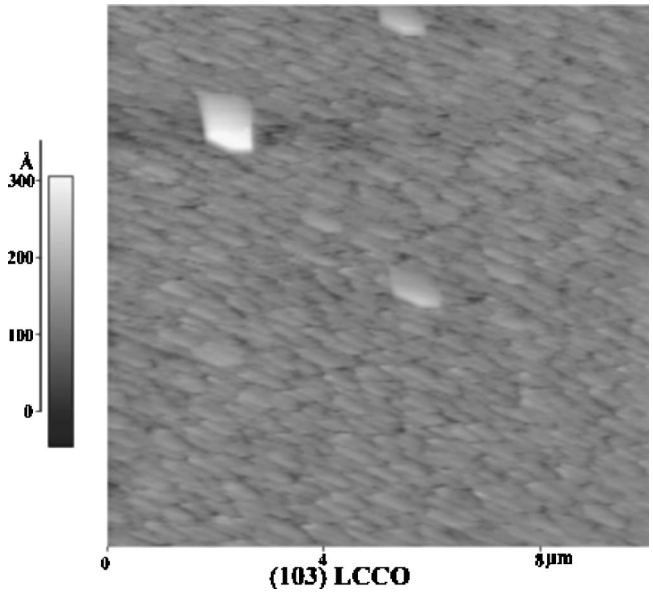

FIG. 2. AFM image of the optimally doped sample (103) LCCO.

and defects in the films that disturb the epitaxial growth and affect the conductance measurement. Figure 1(b) exhibits the XRD θ-2θ pattern of a typical sample which has been grown on a (110) STO substrate under the optimal conditions. The film is (103) oriented, but the XRD intensity of the (103) peak is very weak, corresponding to the poor crystallization for this film.

In order to avoid the unwanted (103) degeneration and the mirror domain in the films, we chose miscut (110) STO as the substrate as used in the fabrication of (103) LSCO thin films by Kwo *et al.*[24] Here, the normal of the (110) surface was rotated around [010] axis about 1°. The surface of the miscut substrate features periodic steps which are designed along (100) planes. The epitaxial growth of LCCO on (100) STO is easier, and results in the same (103) domains in the epitaxial film grown on such miscut (110) STO and the coherent normal direction of the CuO_2 planes. Figure 1(c) shows the XRD θ-2θ pattern of (103) LCCO ($x=0.10$) grown on miscut (110) STO. The XRD intensity of the (103) peak is about of the order of 10^5 and its FWHM is 0.46° [the rocking curve of the (103) peak is shown in the inset], indicating the well-oriented and epitaxial growth of the films. The surface morphology of the sample was tested by atomic force microscopy as shown in Fig. 2. We can see clearly that the (103)-oriented LCCO domains have quite similar orientations indicated by the regular step structure, with few randomly distributed impurity particles on the film surface, which are CuO_x (Cu_2O or CuO?) confirmed by energy-dispersive x-ray analysis as described in our previous paper.[18] Due to the isolated distribution, these particles have no significant contribution to the superconductivity and the normal state transport properties of the films.[18]

Using photolithography and chemical etching techniques, we made each LCCO thin film into a bridge with a width of 100 μm. Then four silver electrodes were deposited on the LCCO film surface with a thickness of $\sim$400 nm *ex situ* by

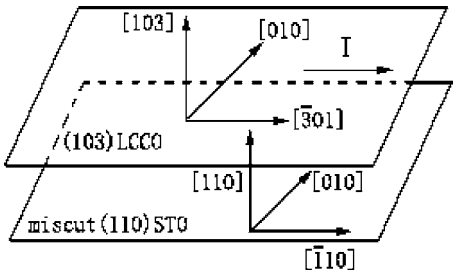

FIG. 3. Sketch map of our measurement configuration. The orientations of STO substrate and LCCO thin films are indexed by the coordinate axes.

magnetron sputtering to assume a conventional four-probe measurement. The patterned bridges on (103)-oriented films are along the [$\bar{3}$01] direction of LCCO epitaxial films, so the currents in our measurements flow along the [$\bar{3}$01] direction of LCCO, and the out-of-plane transport properties can be obtained, as shown in Fig. 3.

III. RESULTS AND DISCUSSION

A. In-plane resistivity

Figure 4 shows the $\rho_{ab}(T)$ curves for (001)-oriented samples with different Ce concentrations. For the optimally doped sample (x=0.10), the $T_{C\ onset}$ and T_{C0} are 28.5 and 27.6 K, respectively, close to the highest T_C recorded of LCCO.[15] In the high-temperature region, the resistivity decreases with the increase of Ce concentration x, which indicates that the density of charge carriers is developed.

The optimally and overdoped LCCO thin films show a metallic behavior in the transport measurements. Unlike the linear temperature dependence in the hole-doped HTSC, such as $YBa_2Cu_3O_7$ (YBCO), the normal state resistivity of LCCO represents a qualitative T^2 relation, which suggests Fermi liquid behavior. To test the T^2 law, we show the curves of the ρ_{ab} versus T^2 of the optimally doped sample in Fig. 5. It is clear that ρ_{ab} has a T^2 trend when the temperature is lower than 190 K, but it deviates from this trend when the temperature is higher. This deviation may be explained in that the T^2 law is deduced from a normal Fermi liquid, while the Cu-O plane is a 2D system. Hence, a modification for the 2D Fermi liquid can be given reasonably as[25,26]

$$\rho(T) = \rho_0 + A(T/T_F)^2 \ln(T_F/T), \tag{1}$$

where ρ_0 is the residual resistance, A is a coefficient, and T_F is the Fermi temperature. We took ρ_0, A, and T_F as the fitting variables. We represent the $\rho \sim T^2 \ln(T_F/T)$ curves for the optimally and overdoped samples as seen in Fig. 6. We have found that the experimental data can be well fitted in the whole measured temperature range above T_C except for the optimally doped sample, which has a deviation from linearity when the temperature is below 80 K. Such linearity behavior is different from the results reported in $Nd_{2-x}Ce_xCuO_4$ by Tsuei *et al.*,[25] where a transition from 3D to 2D was pro-

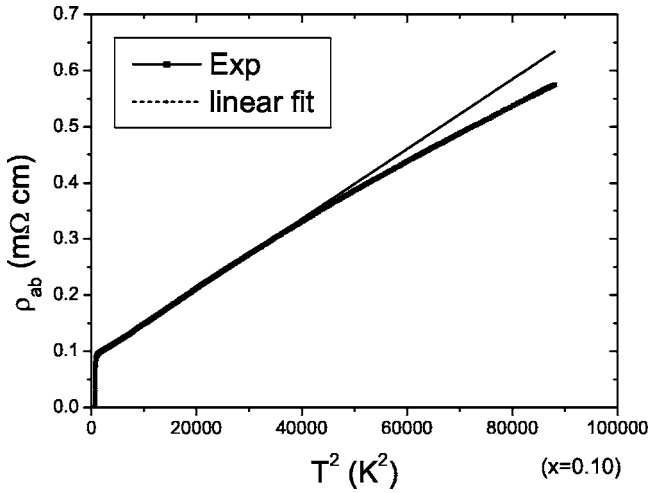

FIG. 5. $\rho_{ab}(T)$ versus T^2 of the optimally doped sample. $\rho_{ab}(T)$ deviates from the T^2 relation when the temperature is higher than 190 K.

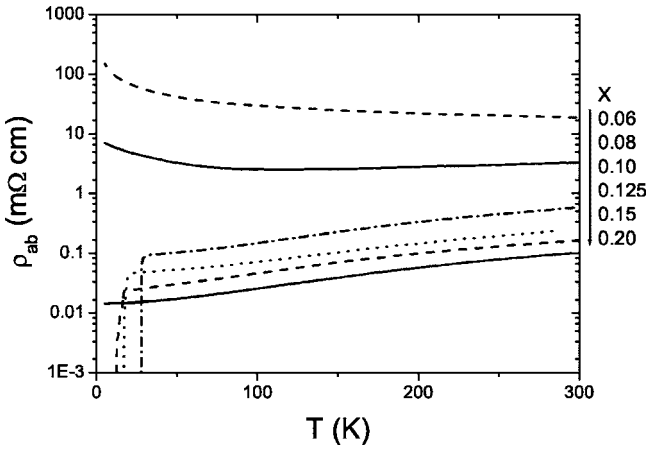

FIG. 4. Temperature dependence of the in-plane resistivity $\rho_{ab}(T)$ for (001) LCCO films with various doping x=0.06–0.20.

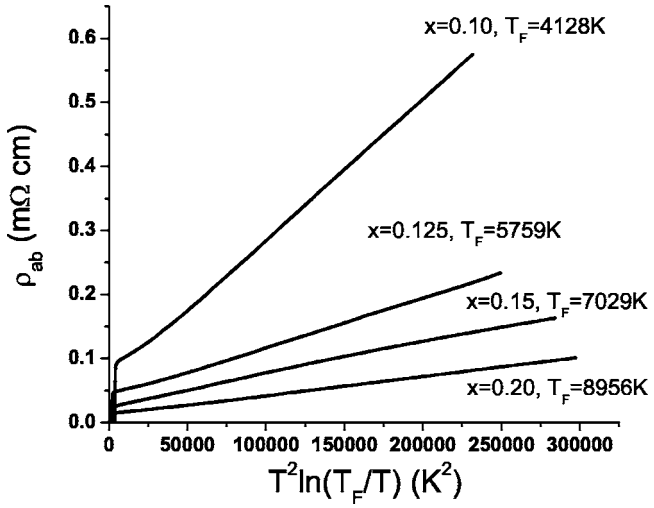

FIG. 6. $\rho_{ab}(T)$ versus $T^2\ln(T_F/T)$ in the whole measured temperature region (5–300 K) for the samples with x=0.10, 0.125, 0.15, 0.20. The fitted values of T_F are shown.

posed with the decrease of temperature. Thus we may suggest that there is no similar 3D-2D phase transition in the LCCO system, at least in the overdoped samples. Further, from this fitting, it is clearly found that with the increase of the doping level x, the values of residual resistance ρ_0 decrease, i.e., from $\sim 50\ \mu\Omega$ cm for $x=0.10$ to $\sim 10\ \mu\Omega$ cm for $x=0.20$, and the values of T_F increase from ~ 4000 K for $x=0.10$ to ~ 9000 K for $x=0.20$. Based on the previous Hall coefficient data of LCCO,[16,18] the density of carriers in LCCO can be estimated to be around $10^{21}-10^{22}$ cm^{-3}, which is two or one orders of magnitude smaller than the value in normal metals. Hence the value of T_F (several thousands kelvin) from our data is reasonable. We also can emphasize that the in-plane transport of LCCO definitely keeps the 2D Fermi liquid feature no matter what the Ce doping concentration when $x \geqslant 0.10$.

In the case of the underdoped sample with $x=0.06$, the ρ_{ab} exhibits a semiconductor behavior in the whole measured temperature range as seen in Fig. 4. While for the sample with $x=0.08$, the resistivity reveals a weak metallic behavior when the temperature is higher than 100 K. In the low-temperature region, upturn behavior occurs. 2D weak localization[21] or Kondo scattering[22] can be taken into account to explain this nonmetallic behavior.

B. *c*-axis resistivity

The transport measurement of the resistivity of the (103)-oriented LCCO thin films was performed by using the configuration as illustrated in Fig. 3. The external current is applied along the $[\bar{3}01]$ direction; then the measured resistivity contains contributions from both c-axis and in-plane components, which can be expressed as[23]

$$\rho_{[\bar{3}01]} = \rho_{ab}\cos^2\theta + \rho_c \sin^2\theta, \tag{2}$$

where ρ_{ab} is the in-plane resistivity and ρ_c is the c-axis resistivity, with $\theta \approx 46°$, the angle between $[\bar{3}01]$ and $[100]$ directions. As mentioned above, both the (103) and (001) samples have the same level of Ce doping, and are deposited in the same conditions and for the same time, so it is reasonable for us to assume that the measured resistivity value from the (001) samples is identical with the ρ_{ab} of (103) samples. Then we can calculate the values of ρ_c by the formula (2).

As seen in Fig. 7, the $T_{C\ onset}$ of the (103)-oriented LCCO thin film is the same as that of the (001)-oriented one. This clearly indicates that both the (103)- and the (001)-oriented thin films have the same essential superconductivity (the $T_{C\ onset}$ is an intrinsic feature of the superconductor), and they may have the same T' phase. However, both $\rho_{[\bar{3}01]}$ (Fig. 7) and ρ_c (Fig. 8) show semiconductorlike behavior (the zero-resistance temperature T_{C0} is lower than 5 K) except for the case of the heavy overdoping of Ce ($x=0.20$). In general, for cuprate superconductors, the semiconductorlike transport behavior may come from quality problems of the sample (imperfect structure, an impure phase, or the underdoping level) or may be an intrinsic feature which may be associated with the localized states of the charge carriers. In the present case, the semiconductorlike transport behavior may not be caused by the sample quality. Just as mentioned above, we grow LCCO thin films on miscut (110) STO substrates to avoid the appearance of the mirror domain, to assure the single-domain growth, which results in minimum domain boundaries. The x-ray diffraction and rocking curve show the good quality of the epitaxial growth of the (103)-oriented thin films. On the other hand, the semiconductorlike transport behavior occurs not only in the case of underdoped samples, but also in the optimally and overdoped samples (the weak metallic behavior just appears in the heavily overdoped sample, $x=0.20$). Hence the dopant concentration is also not the reason for the semiconductorlike feature of ρ_c. Therefore, such behavior in ρ_c should be a result of intrinsic features, and it may be possibly due to the coupling between Cu-O planes, because the transport along the c axis must be dominated by the coupling strength of the Cu-O planes and the corresponding charge carrier distribution in the c-axis direction. Due to the weak coupling or strong 2D characteristic, the transport passing along the c-axis direction should be dominated by the hoping conductance mode and results in a lower T_{C0} though the $T_{C\ onset}$ is the same as that in the (001)-oriented thin film. In the heavily overdoped case $x=0.20$, weak metallic transport behavior appears, which may

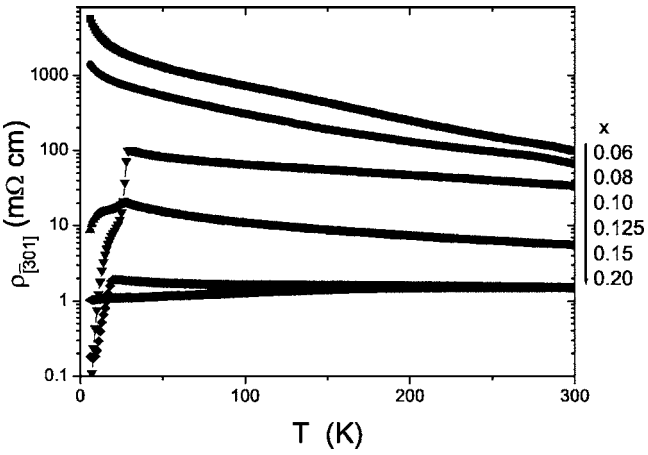

FIG. 7. The measured raw data of the temperature dependence of $\rho_{[\bar{3}01]}$ for (103) LCCO with $x=0.06-0.20$.

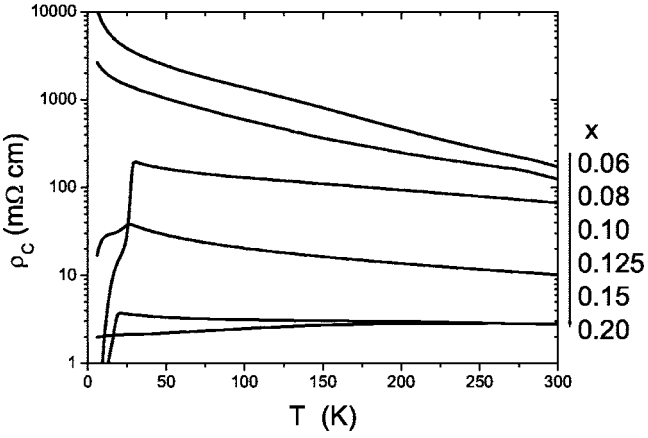

FIG. 8. The calculated values of the temperature dependence of ρ_c from the expression (2) for (103) LCCO with $x=0.06-0.20$.

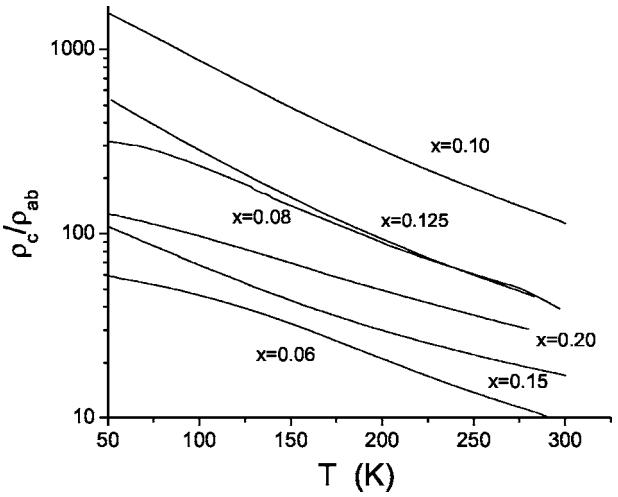

FIG. 9. The temperature dependance of the anisotropy factor of the resistivity for LCCO films with $x=0.06$, 0.08, 0.10, 0.125, 0.15, and 0.20.

be due to the change of the distribution of the charge carriers with higher density in the c-axis direction. In fact, in this heavily overdoped case, the superconductivity naturally disappears and no evaluation of T_C can be made. The transport behavior due to the coupling between Cu-O planes can be understood further in the discussion of anisotropy of LCCO later.

On the other hand, the strain effect between the films and the substrates should also be a factor that influences the transport properties of the superconducting thin film. For the (103)-oriented LCCO thin film, the Cu-O planes are not parallel to the substrate plane but have an angle ($\sim 46°$) to it. Then all Cu-O planes near the interface possibly meet the interface effect, and the strain effect in the (103)-oriented thin film may be stronger than in the (001)-oriented one. Such strain effect does not mean a change of the structure, but induces lattice distortion in the interface, which has an interaction with the charge carriers, and possibly leads to the formation of localized states in the interface. This should influence both ρ_{ab} and ρ_c, but mainly ρ_c in the (103)-oriented thin film, and give a contribution to the semiconductor-like transport behavior.

Figure 9 shows the temperature dependence of the anisotropy factor (ρ_c/ρ_{ab}) on Ce concentration. The ratio is in the range from 10 to 1500, indicating a very large anisotropy and a very strong 2D feature, i.e., there is a very weak coupling between Cu-O planes. The ratio ρ_c/ρ_{ab} of all samples increases with decrease of the temperature by an order of magnitude from 300 to 50 K. Such anisotropic features and temperature dependence of LCCO thin films are similar but much stronger than those of NCCO thin films,[13] implying the rather perfect epitaxial growth of our LCCO thin films. For comparison, the anisotropy factor of the present LCCO thin films is smaller than that of the NCCO single crystal[27] (while no comparison can be made for the LCCO thin film and single crystal since a single crystal of LCCO cannot be prepared at present). For this difference, the interface effect should be considered. As mentioned above, the interface (between the film and the substrate) effects (e.g., the strain effect) may suppress the conductance in both the Cu-O plane and the c-axis direction; then ρ_c/ρ_{ab} will be smaller. Such discussion has been addressed for NCCO and other electron-doped thin films with different orientations [other than (001)].[28]

For the three samples in the superconducting doping region ($x=0.10, 0.125, 0.15$), the values of ρ_c/ρ_{ab} show similar temperature dependence. The optimally doped sample ($x=0.10$) has the largest anisotropy coefficient, while the sample with more overdoped Ce ($x=0.15$) has the smallest anisotropy in these three samples. A similar correlation was also observed in NCCO.[12,13] The two underdoped samples with $x=0.06$ and 0.08 have smaller ρ_c/ρ_{ab} values, while the anisotropy of the sample with $x=0.06$ is smaller than that of the sample with $x=0.08$. This is because the ρ_{ab} of the sample with $x=0.06$ is much larger than that of the sample with $x=0.08$. In particular, as mentioned above, the ρ_{ab} of the sample with $x=0.06$ exhibits a semiconductor behavior, while in the sample with $x=0.08$, ρ_{ab} shows a weak metallic behavior in the higher-temperature region. Hence it is clear that the Ce doping concentration plays an important role in the anisotropy of LCCO thin films. Nevertheless, it should be noted that the strongest anisotropy is found in the LCCO thin film with the optimal doping of Ce, corresponding to the strongest superconductivity. Further work is still necessary to clarify the intrinsic anisotropy of LCCO, especially in single crystals, and is expected in the future.

IV. CONCLUSION

We have grown $La_{2-x}Ce_xCuO_4$ ($0.06 \leqslant x \leqslant 0.20$) thin films epitaxially on (001) and miscut (110) STO substrates. The films are respectively (001) and (103) oriented with single domain, giving ideal ways to investigate the in-plane and out-of-plane transport properties (the anisotropic transport) of LCCO. In the underdoped case, the ρ_{ab} of (001)-oriented films reveals a transition from a metallic to a nonmetallic state with decreasing temperature. While the c-axis resistivity always remains in the nonmetallic state in the whole measured temperature range except for the heavily overdoped films ($x=0.20$). For the optimally and overdoped (001) LCCO films, the ρ_{ab} clearly show T^2 dependence with a logarithmic correction, i.e., a 2D Fermi liquid behavior can be suggested. It should be particularly noted that the anisotropy is apparently dominated by the Ce doping concentration, and the largest anisotropy ratio of 1500 at 50 K is achieved for the optimal Ce doping, indicating the strongly 2D feature of the superconductivity for the LCCO system.

ACKNOWLEDGMENTS

The authors would like to thank H. Chen, S. L. Jia, and W. W. Huang for their measurement support and informative discussions. This work is supported by grants from the State Key Program for Basic Research of China and the National Natural Science Foundation.

*Electronic address: brzhao@aphy.iphy.ac.cn

[1] A. S. Alexandrov, V. V. Kabanov, and N. F. Mott, Phys. Rev. Lett. **77**, 4796 (1996).
[2] P. Prelovšek, A. Ramšak, and I. Sega, Phys. Rev. Lett. **81**, 3745 (1998).
[3] L. B. Ioffe and A. J. Millis, Phys. Rev. B **58**, 11631 (1998).
[4] M. Giura, R. Fastampa, S. Sarti, and E. Silva, Phys. Rev. B **68**, 134505 (2003).
[5] T. Ito, Y. Nakamura, and S. Ishibashi, Nature (London) **350**, 596 (1991).
[6] S. J. Hagen, T. W. Jing, Z. Z. Wang, J. Horvath, and N. P. Ong, Phys. Rev. B **37**, 7928 (1988).
[7] S. Martin, A. T. Fiory, R. M. Fleming, L. F. Schneemeyer, and J. V. Waszczak, Phys. Rev. B **41**, 846 (1990).
[8] Y. Ando, G. S. Boebinger, A. Passner, T. Kimura, and K. Kishio, Phys. Rev. Lett. **75**, 4662 (1995).
[9] Y. Nakamura and S. Uchida, Phys. Rev. B **47**, R8369 (1993).
[10] Beom-hoan O and J. T. Markert, Phys. Rev. B **47**, 8373 (1993).
[11] M. A. Crusellas, J. Fontcuberta, and S. Piñol, Physica C **235-240**, 1401 (1994).
[12] S. L. Copper and K. E. Gray, in *Physical Properties of High Temperature Superconductors* (World Scientific, Singapore, 1994), p. 74.
[13] A. I. Ponomarev, T. B. Charikova, A. N. Ignatenkov, A. O. Tashlykov, and A. A. Ivanov, Low Temp. Phys. **30**, 885 (2004).
[14] T. Yamada, K. Kinoshita, and H. Shibata, Jpn. J. Appl. Phys., Part 2 **33**, L168 (1994).
[15] M. Naito and M. Hepp, Jpn. J. Appl. Phys., Part 2 **39**, L485 (2000).
[16] A. Sawa, M. Kawasaki, H. Takagi, and Y. Tokura, Phys. Rev. B **66**, 014531 (2002).
[17] K. Oka, H. Shibata, S. Kashiwaya, and H. Eisaki, Physica C **388-389**, 389 (2003).
[18] L. Zhao, H. Wu, J. Miao, H. Yang, F. C. Zhang, X. G. Qiu, and B. R. Zhao, Semicond. Sci. Technol. **17**, 1361 (2004).
[19] A. Manthiram and J. B. Goodenough, J. Solid State Chem. **87**, 402 (1990).
[20] M. Naito, A. Tsukada, T. Greibe, and H. Sato, cond-mat/0209277 (unpublished).
[21] P. Fournier, J. Higgins, H. Balci, E. Maiser, C. J. Lobb, and R. L. Greene, Phys. Rev. B **62**, R11993 (2000).
[22] T. Sekitani, M. Naito, and N. Miura, Phys. Rev. B **67**, 174503 (2003).
[23] M. Suzuki, K. Moriwaki, and T. Murakami, Jpn. J. Appl. Phys., Part 2 **26**, L1921 (1987).
[24] J. Kwo, R. M. Fleming, H. L. Kao, D. J. Werder, and C. H. Chen, Appl. Phys. Lett. **60**, 1905 (1992).
[25] C. C. Tsuei, A. Gupta, and G. Koren, Physica C **161**, 415 (1989).
[26] G. F. Giuliani and J. J. Quinn, Phys. Rev. B **26**, 4421 (1982).
[27] Y. Onose, Y. Taguchi, K. Ishizaka, and Y. Tokura, Phys. Rev. B **69**, 024504 (2004).
[28] Michio Naito (private communication).